Quasiparticle echoes in scanning tunneling microscopy

Sumiran Pujari and C. L. Henley
Department of Physics, Cornell University, Ithaca, New York 14853-2501, USA
(Received 12 November 2009; revised manuscript received 31 May 2010; published 13 July 2010)

It is shown that the local density of states, measured in a scanning tunneling microscopy (STM) experiment, at a single tip position contains oscillations as a function of *energy*, due to quasiparticle interference, which is related to the positions of nearby scatterers. We propose a method of STM data analysis based on this idea, which can be used to *locate* the scatterers. In the case of a superconductor, the method can potentially distinguish the nature of the scattering by a particular impurity.

DOI: 10.1103/PhysRevB.82.035109 PACS number(s): 74.25.Jb, 72.10.Fk, 73.20.At, 74.72.−h

I. INTRODUCTION

Scanning tunneling microscopy (STM), which measures the "local density of states" (LDOS) as a function of position and energy set by the bias voltage, has opened the door to imaging the subnanoscale topography and electronic structure of materials, including normal metals[1] and especially cuprate superconductors.[2–9]

The dispersion relations of (Landau or Bogoliubov) quasiparticles may be extracted from STM data on normal metals[10,11] and superconductors,[12] via the inverse method called Fourier transform scanning tunneling spectroscopy (FT-STS),[10,12] or directly in real space.[11] This technique is based on the fact that impurities produce spatial modulations of the LDOS in their vicinity-standing waves in the electronic structure that generalize the Friedel oscillations found in metals at the Fermi energy. In the cuprates BSCCO (bismuth strontium calcium copper oxide) and CaCuNaOCl,[12] experiments showed these quasiparticle oscillations were dominated by eight wave vectors that connect the tips of "banana-shaped" energy contours in reciprocal space, the so-called Octet model as explained theoretically.[13] For optimally doped samples, the dispersion inferred from these wave vectors agrees well with *d*-wave BCS theory indicating the existence of well-defined BCS quasiparticles in this regime.

The central observation of this paper is that the same Friedel-type oscillations of the LDOS, analyzed in the space/momentum domain by FT-STS, are also manifested in the energy/time domain. Our analysis shows that the small impurity-dependent modulations of the LDOS have a period, in energy, inversely proportional to the time required by a quasiparticle wave packet to travel to the nearby impurities and backhence we call it "quasiparticle echo." From this, in principle, one can determine the location and (in a superconductor) the nature of the point scatterers in a particular sample.

The basic idea of the LDOS modulations may be understood semiclassically. The LDOS $N(\vec{r};\omega)$ is defined as $-(1/\pi)\mathrm{Im}\, G(\vec{r},\vec{r};\omega)$, the time Fourier transform of the local (retarded) Green's function $G(\vec{r},\vec{r};t)$. Imagine a bare electron wave packet (centered on energy ω) is injected at time $t=0$ at point $\vec{r}$ in a two-dimensional material: the Green's function expresses its subsequent evolution. Assuming there are well-defined quasiparticles at this energy with dispersion $E(\vec{k})$; then for every wave vector $\vec{k}$ on the energy contour $E(\vec{k})=\omega$, the wave packet has a component spreading outward at the group velocity $\vec{v}_g(\vec{k}) \equiv \nabla_{\vec{k}} E(\vec{k})/\hbar$. When this ring reaches an impurity at $\vec{r}_{\mathrm{imp}}$, it serves as a secondary source and the reflected wave packet arrives at the "echo time"

$$T_e \equiv 2\frac{|\vec{R}|}{|\vec{v}_g(\vec{k})|} \tag{1}$$

for the $\vec{k}$ such that $\vec{v}_g(\vec{k}) \| \vec{R} \equiv \vec{r}_{\mathrm{imp}} - \vec{r}$. This creates a sharp peak at $t=T_e$ in $G(\vec{r},\vec{r};t)$ [see Fig. 1(d)] and hence modulations as a function of ω in its Fourier transform $N(\vec{r};\omega)$ with period $\Delta\omega = 2\pi\hbar/T_e$.[14] Generically, for a particular impurity direction, $|\vec{v}_g|$ varies with energy, so the modulation in $\delta N(\omega)$ due to the impurity is "chirped" correspondingly.

II. NORMAL METAL

We illustrate the quasiparticle echo first by a numerical calculation for a normal metal, defined by the lattice Schrodinger equation for the wave function u_i on site i

$$\sum_j (t_{ij} + \mu_i \delta_{ij}) u_i = E u_i. \tag{2}$$

Here the $t'_{ij}s$ are intersite hoppings and the μ_i's are on-site potentials (including the chemical potential); in this paper, we assume they are translationally invariant except at discrete (and dilute) impurity sites. We take the specific case of nearest-neighbor hopping t at half-filling, so the dispersion is $\epsilon(k_x,k_y) = -2t(\cos k_x + \cos k_y)$, and we place one (repulsive site potential) impurity at the origin. To numerically calculate the LDOS, we used the Recursion method,[15] which is well-suited for cases without translational symmetry.

Figure 1(a) shows the impurity case LDOS which has echo oscillations on top of what otherwise would have been clean case LDOS, visible along the sides of the peak. Note that, for us to see more than one oscillation within the bandwidth, the impurity must be at least several sites away; hence the oscillations always have small amplitude and are best viewed by subtracting the clean LDOS. Throughout the paper, energy is in units of t and time in units of t^{-1} with $t=1$ and $\hbar=1$.

For a given energy ω, we define $\Delta\omega(\omega)/2$ as the separation of the zeroes that bracket ω in the (subtracted) $\delta N(\omega)$

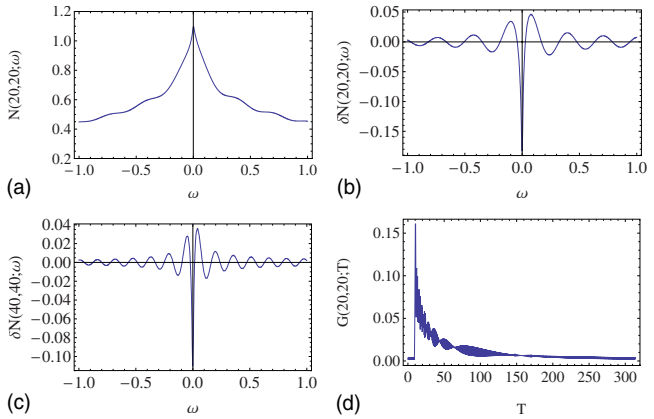

FIG. 1. (Color online) LDOS as a function of energy, showing oscillations due to quasiparticle echoes. (a) LDOS at a point $20\sqrt{2}$ away from a point impurity along the [1,1] direction (lattice constant=1). (b) Corresponding LDOS after subtracting the clean LDOS: $\delta N(20,20;\omega)$, (c) $\delta N(40,40;\omega)$, and (d) magnitude of local Green's function as a function of time: $|G(20,20;T)|$. The singularity appears at time $T_e/2$, where T_e is given by Eq. (1). As we change the distance along this direction, the shortest echotime changes in proportion in accordance with our semiclassical expectations. Energy (ω) are in units of t and time (T) in units of T^{-1}.

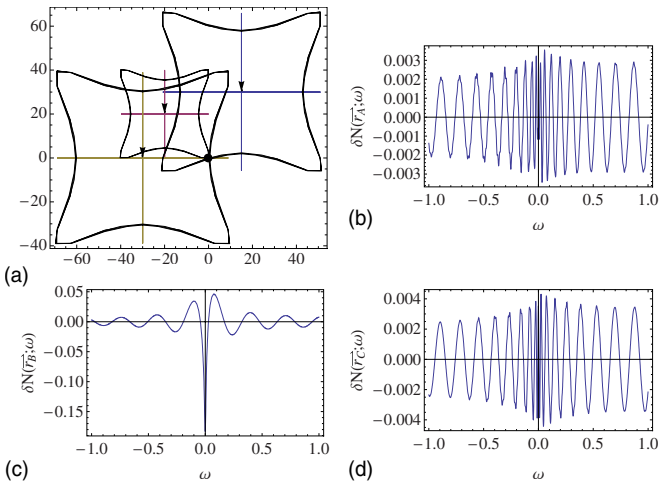

FIG. 2. (Color online) (a) Schematic of few measurements around an impurity. The arrowheads represent the STM Tip positions. The x and y axes are in units of lattice constant which is set to 1. After measurement, we get (b) $\delta N(\vec{r}_A;\omega)$, (c) $\delta N(\vec{r}_B;\omega)$, and (d) $\delta N(\vec{r}_C;\omega)$. Extracting the echotimes for each measurement at $\omega=0.7t$, we locate the impurity, shown as a black dot, in the first panel. Note, that the locus of impurity locations changes with ω, and is of the shape shown only at $\omega=0.7t$. Energy (ω) are in units of t.

trace, and let $T_e(\omega)\equiv 2\pi\hbar/\Delta\omega(\omega)$. We chose $E=0.7t$ and $\vec{R}$ in the [1,1] direction, for which the group velocity is $v_g=2.785t/\hbar$. Then, using $\delta N(20,20;\omega)$, $\delta N(30,30;\omega)$, and $\delta N(40,40;\omega)$ [the first and last trace of these are shown in Figs. 1(c) and 1(d)], we read off $\Delta\omega/2=0.1545$, 0.103, and 0.077, from which $v_g T_e/2=20.04\sqrt{2}$, $30.05\sqrt{2}$, and $40.22\sqrt{2}$, respectively. The proportionality between the oscillation rate and the actual distance confirms the semiclassical explanation of these modulations.

A. "Echolocation" of Impurity

Using these quasiparticle echoes, we can locate the position of impurities by measuring the LDOS wiggles at a few points in the vicinity. At each point, we extract the wiggle period $\Delta\omega$ and hence the echo time $T_e\equiv 2\pi/\Delta\omega$. Then Eq. (1) defines a locus of possible impurity locations, $\{\vec{v}_{group}(\vec{k})T_e/2:\epsilon(\vec{k})=\omega$. The intersection of the loci from STM spectra taken at multiple points $\vec{r}$ will locate $\vec{r}_{\rm imp}$ uniquely. Furthermore, via a more exact derivation of the LDOS modulations (see below), the amplitude of the LDOS modulations tells the scattering strength of the impurities (in Born approximation they are proportional to each other). Once an impurity has been pin-pointed, the higher energy STM spectrum at that point may independently identify the chemical nature of the impurity, e.g., in cuprates[16] and thus may reveal which kinds of impurities are important for the scattering of quasiparticles.

As a test, we evaluated the subtracted LDOS at three points $\vec{r}_A=(-30,0)$, $\vec{r}_B=(-20,20)$, and $\vec{r}_C=(15,30)$, with the impurity at $\vec{r}=0$. From the half-periods of the wiggles at energy=$0.7t$, (extracted as before) we found the respective echo times $T_A=39.9$, $T_B=20.4$, and $T_C=36.7$. The three scaled loci (scaled by half the respective echotimes), shown in Fig. 2(e), intersect at (0,0) as can be seen graphically. Since we are inferring echo times and then converting them to distances in space, this method is a form of "echolocation," analogous to the well-known examples in radar or of sonar echolocation by bats and dolphins.[17] A careful analysis of errors in estimation of echo times can be done to extract errors in echolocation as well.

We emphasize again that this method locates impurities *as seen by* quasiparticle interference and, hence, is different from the well-known methods of locating impurities by their local spectral signatures. Even though we may or may not have a detailed understanding of the STM spectra near the impurity, this method is not limited to it as it uses far-from-impurity measurements to locate the impurity. Hence, potentially, this method can overcome the limitations of and/or confirm the predictions for impurities' recognition from their spectral signatures or comparisons with near-impurity data (e.g., see Sec. IX of Ref. 18 in context of cuprates)

B. Analytic derivation

Adopting the T-matrix formalism, we can obtain an analytic form for the LDOS modulations. Formally, the difference in dirty LDOS and clean LDOS for a single point impurity is given by

$$\delta N(\vec{r};\omega) = -\frac{1}{\pi}\mathrm{Im}[G_0(\vec{r}-\vec{r}_{\rm imp};\omega)T(\omega)G_0(\vec{r}_{\rm imp}-\vec{r};\omega)], \tag{3}$$

where $G_0(\vec{r},\vec{r}_{\rm imp};\omega)\equiv G_0(\vec{r}-\vec{r}_{\rm imp};\omega)\equiv G_0(\vec{R};\omega)$ is the free propagator; LDOS modulations are due to interference between the two G_0 factors.

$$G_0(\vec{R};\omega) = \lim_{\delta\to 0^+} \int_{\mathrm{BZ}} \frac{dk_x dk_y}{(2\pi)^2} \frac{e^{i\vec{k}\cdot\vec{R}}}{\omega + i\delta - \epsilon(\vec{k})}. \tag{4}$$

The integrand is singular all along the energy contour $\epsilon(\vec{k}) = \omega$, which we also parametrize as $\vec{k}_\epsilon(s)$, where s is the arc length in reciprocal space. By the change in variables $z \equiv e^{ik_y}$ we convert the inner (k_y) integral to a complex contour integral in the z plane [rewriting $\epsilon(k_x,k_y)$ as an analytic function of z]; for k_x values found on the energy contour, the z path encounters two poles, one inside and one outside, depending on the sign of δ. Extracting the residue and absorbing factors, we get

$$G_0(\vec{R};\omega) = \frac{1}{2\pi i} \oint \eta(s) ds \frac{e^{i\vec{k}_\epsilon(s)\cdot\vec{R}}}{\hbar v_g[\vec{k}_\epsilon(s)]} + G_{\mathrm{nonsingular}}, \tag{5}$$

where $\eta(s)=1$ on the half of the energy contour where $\mathrm{sgn}(\delta)=\mathrm{sgn}[|\vec{v}_g(\omega,s)|]$ and zero on the other half. The nonsingular term $G_{\mathrm{nonsingular}}$ comes from the integrals over k_y which do *not* cross the energy contour.

At large $\vec{R}$, the two-dimensional Brillouin zone (BZ) integration will be dominated by those $\vec{k}$ (Ref. 19) on the energy contour where the phase in the numerator is stationary, i.e., $\vec{v}_g(\vec{k}) \| \vec{R}$: let us call such a point $\vec{k}_{\vec{R}}$ (so it is a function of the direction $\hat{R}$ and of ω). Using standard formulas of the stationary phase approximation[20] we get asymptotically

$$G_0(\vec{R};\omega) = \frac{-ie^{i\pi/4}}{v_g} \sqrt{\frac{1}{2\pi\kappa|\vec{R}|}} e^{i\vec{k}_{\vec{R}}(\vec{R},\omega)\cdot\vec{R}}. \tag{6}$$

Here κ^{-1} is the curvature $d^2\vec{k}_\epsilon/ds^2$ of the energy contour at $\vec{k}_{\vec{R}}$.

Using Eqs. (1) and (3), we finally get

$$\delta N(\omega) = \frac{T}{2\pi^2 v_g^2 \kappa R} \cos[2\vec{k}_{\vec{R}}(\vec{R},\omega)\cdot\vec{R}]. \tag{7}$$

valid in the limit of a distant impurity. (All factors are actually functions of $\vec{R}$ and ω: these arguments are shown only in the rapidly varying factors.) As we change ω to $\omega+\delta\omega$ keeping $\vec{R}$ fixed, the chain rule gives $\vec{k}_{\vec{R}}(\omega+\delta\omega)-\vec{k}_{\vec{R}}(\vec{R},\omega) = v_g^{-1}\delta\omega\hat{R}$ so, with $\phi=\vec{k}_{\vec{R}}\cdot\vec{R}$, we get

$$\cos[2\vec{k}_{\vec{R}}(\vec{R},\omega+\delta\omega)\cdot\vec{R}] \to \cos(\phi + T_e\delta\omega). \tag{8}$$

This confirms the simple semiclassical prediction $\Delta\omega = 2\pi/T_e$ [see Eq. (1)] for the modulation period due to echoes. The same quasiparticle interference is responsible for the spatial oscillations evident in Eq. (7) and the energy oscillations in Eq. (8).

III. ECHOES IN SUPERCONDUCTORS

Additional relevant issues arise in case of superconductors. To discuss these, we use a mean-field Bogoliubov-DeGennes (BDG) Hamiltonian with/without a single point impurity as shown below.

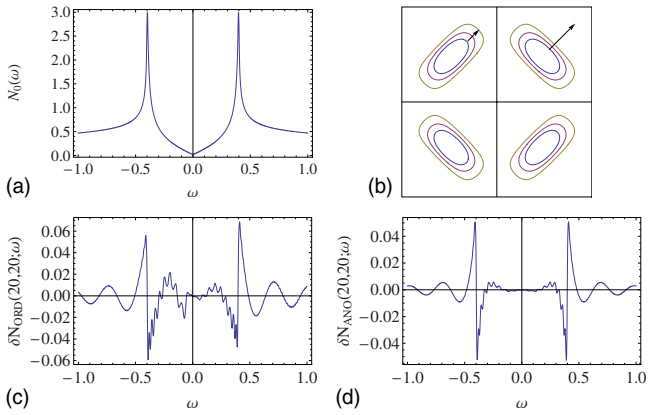

FIG. 3. (Color online) Quasiparticle echoes in a d-wave SC. (a) No impurity $N_0(\omega)$ showing the d-wave gap, (b) a caricature of the two different group velocities along (1,1) direction for d-wave Bogoliubov dispersion in the first Brillouin zone. The x and y axes correspond to k_x and k_y, respectively, and are in units of inverse lattice constant (which is set to 1) and range from $[-\pi,\pi]$. (c) $\delta N_{\mathrm{ORD}}(20,20;\omega)$ for an ordinary impurity and (d) $\delta N_{\mathrm{ANO}}(20,20;\omega)$ for an anomalous impurity. Energy (ω) are in units of t.

$$\sum_j \begin{bmatrix} t_{ij}+\mu_i\delta_{ij} & \Delta_{ij} \\ \Delta_{ij}^* & -t_{ij}-\mu_i\delta_{ij} \end{bmatrix} \begin{bmatrix} u_i \\ v_i \end{bmatrix} = E \begin{bmatrix} u_i \\ v_i \end{bmatrix}, \tag{9}$$

where we are using a lattice formulation of BDG equations. The u_is and v_is represent particle and hole amplitudes on site i, t_{ij}s and μ_is represent the intersite hoppings and site chemical potentials, respectively, and Δ_{ij} represent the off-diagonal order parameter amplitude. We discuss d-wave superconductors (dSCs) to highlight this method's application to cuprates. For dSCs, Δ_{ij} is nonzero only on nearest-neighbor bonds and $\Delta_{\hat{i},\hat{i}\pm\hat{x}} = -\Delta_{\hat{i},\hat{i}\pm\hat{y}}$ because of the d-wave nature. Our normal state is the same nearest-neighbor tight-binding model on the square lattice with $t=1$ and off-diagonal hopping amplitudes set to $|\Delta|=0.1$. The Recursion method was extended to superconductors in Ref. 21 and is used for our numerics. In Figs. 3(c) and 3(d), we show the LDOS [after subtracting the clean LDOS shown in Fig. 3(a)] at $20\sqrt{2}$ distance from an impurity along the (1,1) direction for the case of a potential scatterer and an anomalous pair potential scatterer (which scatters an electron into a hole and vice versa), respectively.

In contrast to the normal case, there are two different wiggles: a fast one and a slow one. The reason for this is that the dSC quasiparticle dispersion gives rise to two different group velocities in the (1,1) direction.[22] We also note that the fast wiggles exist only within the gap while the slow wiggles are both inside and outside the gap. In Fig. 3(b), we show the constant energy contours for the quasiparticle dispersion given by $E(\vec{k}) = \sqrt{\epsilon(\vec{k})^2 + \Delta(\vec{k})^2}$, the gradient of which is the quasiparticle group velocity. From Fig. 3(b), we see that along (1,1), the banana-shaped energy contours in the first and third quadrants give one velocity (which corresponds to the slow wiggles) while the contours in the second and fourth quadrants give a slower velocity (which corresponds

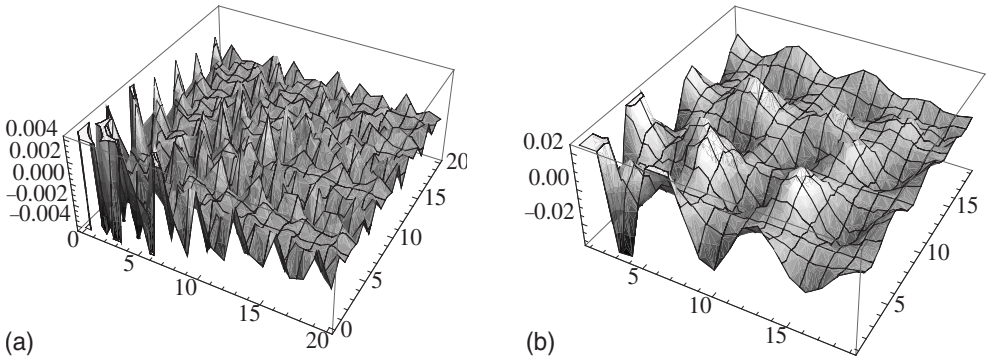

FIG. 4. Shown are the $\delta N(\vec{R};\omega=0.35t)$ around an ordinary and d-wave anomalous impurity in the Born limit over a grid of $(0,20)\times(0,20)$ with other quadrants related by symmetry. The x and y axes are in units of lattice constant which is set to 1. (a) δN_{ORD} and (b) $\delta N_{\text{d-ANO}}$. A subgap value of $\omega=0.35t$ was chosen arbitrarily.

to the fast wiggles). For $E>|\Delta|$, there are no longer banana contours so we get only one group velocity (similar to the normal case) and hence only one kind of wiggle is seen in Figs. 3(c) and 3(d) outside the cusps.

Once the impurity is *located* using the loci intersection method described before, one can study the LDOS data around the impurity to infer the impurity's strength and whether it is ordinary (magnetic/nonmagnetic) (cf. Ref. 18 and references therein) or anomalous.[23] This distinction is already visible in individual spectra: provided the normal state is particle-hole symmetric, one gets particle-hole *symmetric* echo oscillations δN_{ANO} from an anomalous impurity, since it scatters electrons into holes and vice versa [Fig. 3(d)]; this is *not* the case for δN_{ORD} from an ordinary impurity [Fig. 3(c)].

A second diagnostic distinguishing (nonmagnetic) ordinary scatterers from anomalous ones is the real-space pattern of the surrounding standing waves in the LDOS, which is best seen in Born approximation. In this weak impurity limit, the impurity T matrix is of the form (in the 2×2 Nambu notation) $U_{\mathrm{imp}}\tau_3$ or $\Delta_{\mathrm{imp}}\tau_1$ for the ordinary or anomalous cases, respectively. Then the echo oscillations take the respective forms

$$\delta N_{\mathrm{ORD}} \propto U_{\mathrm{imp}}(G_{11}^2 - G_{12}^2); \quad \delta N_{\mathrm{ANO}} \propto \Delta_{\mathrm{imp}}(2G_{11}G_{12}). \tag{10}$$

Here, the G_{ij}s are the matrix elements of the usual free propagator $G_0(\vec{k};\omega)=[\omega^2-E(\vec{k})^2]^{-1}[\omega+\epsilon(\vec{k})\tau_3+\Delta(\vec{k})\tau_1]$ thus in real space

$$G_0(\vec{R};\omega) = \frac{\pi i}{(2\pi)^2}\oint \eta(s)\frac{ds}{2}g[\vec{k}(s,\omega)] + G_{\mathrm{nonsingular}}, \tag{11}$$

where $g(\vec{p};\vec{R},\omega)\equiv 1+\frac{1}{\omega}[\epsilon(\vec{p})\tau_3+\Delta(\vec{p})\tau_1]$. We can carry out the stationary phase approximation as before but instead we numerically calculated the propagator using Eq. (11) since we are interested in LDOS information around (close) to the impurity.

In the panels of Fig. 4, we show δN around an impurity in the Born limit over a grid of 20×20 lattice points (shown one quadrant with others related by symmetry). We see that some of the *real-space* oscillations, present in case of the ordinary impurity, are suppressed in the case of a d-wave anomalous impurity. This is the same effect as the suppression of certain "octet" vectors[12,13] for the case of d-wave anomalous impurity as argued in Eq. 10 of Ref. 23 and the following paragraph. These differences in the real-space oscillations around the impurity for ordinary and d-wave anomalous cases can be exploited to distinguish impurities

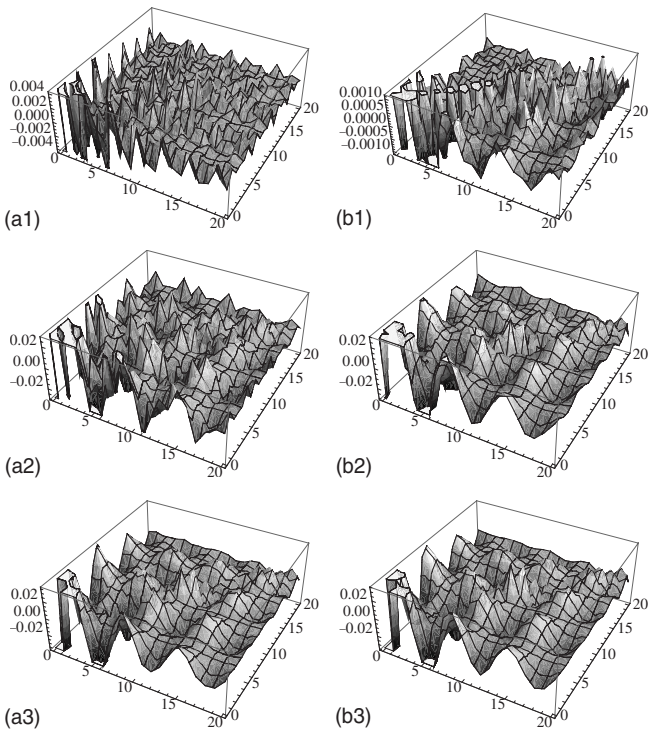

FIG. 5. Shown are the $\delta N(\vec{R};\omega=0.35t)$ around an ordinary and s-wave anomalous impurity for varying impurity strengths (from a weak impurity in the Born limit to a strong impurity in the unitary limit) over a grid of $(0,20)\times(0,20)$ with other quadrants related by symmetry. The x and y axes are in units of lattice constant which is set to 1. (a) δN_{ORD} and (b) $\delta N_{\text{s-ANO}}$, and (1) $0.1t$, (2) t, and (3) $5t$ for impurity strengths. A subgap value of $\omega=0.35t$ was chosen arbitrarily.

once they are located. This agreement of suppression of some oscillations in our real-space calculations and the Fourier-space analysis of Ref. 23 illustrates how the real-space quasiparticle interference oscillations and our energy-domain echoes are complementary manifestations of the same phenomenon.

In the panels of Fig. 5, we illustrate another point regarding distinguishing ordinary and anomalous impurities using ordinary and *s*-wave anomalous point impurities. We see that the differences between the two kinds of impurities decrease with increasing impurity strength with them being virtually indistinguishable in the strong impurity limit. This observation is pertinent to STM phenomenology since it tells us that if the impurity is strong, then STM is effectively unable to tell between impurities and one has to be careful about making any conclusions on the ordinariness/anomalousness of the impurity. This observation can be understood by looking at the expression of the full impurity T matrix for a local impurity,[24] which is $T(\omega)=U[1-G_0(0;\omega)U]^{-1}$, where U and G_0 are understood to be 2×2 Nambu matrices. We see that in the Born limit, the identity matrix in the bracket dominates and thus the T matrix is effectively U as expected. On the other extreme, as the impurity becomes stronger and stronger, the G_0U will start dominating over the identity, thus making the T matrix effectively $G_0(0;\omega)^{-1}$ which is independent of the impurity matrix. This is why Figs. 4(a3) and 4(b3) look practically the same.

IV. CONCLUSION AND DISCUSSION

In conclusion, we have proposed a method of STM data analysis in the energy domain as a phenomenological tool for the study of real materials, complementary to FT-STS. Since it is based on the *same* quasiparticle interference effects already used successfully in FT-STS, we have confidence that the signals will be observable. They should be particularly strong in materials with an energy-dependent group velocity in some range of energies, such as *d*-wave superconductors and also graphene.[25]

Since the echo analysis can be done in local patches of the sample (unlike FT-STS which Fourier transforms over a larger region), we can *locally* verify the existence of quasiparticles at various energies through QPI. In particular, in cuprates, echoes might be used to check the hypothesis of quasiparticle extinction[26] above a certain energy. Furthermore, we have argued that echo analysis might reveal the nature of specific impurities[27] in a sample, information which hitherto was (at best) known statistically.

ACKNOWLEDGMENTS

We thank S. C. Davis, A. V. Balatsky, and P. J. Hirschfeld for discussions. S.P. thanks Stefan Baur for valuable help in using MATHEMATICA. This work was supported by NSF under Grant No. DMR-0552461.

[1] M. F. Crommie, C. P. Lutz, and D. M. Eigler, Science **262**, 218 (1993); Nature (London) **363**, 524 (1993).
[2] A. Yazdani, C. M. Howald, C. P. Lutz, A. Kapitulnik, and D. M. Eigler, Phys. Rev. Lett. **83**, 176 (1999).
[3] E. W. Hudson, S. H. Pan, A. K. Gupta, K.-W. Ng, and J. C. Davis, Science **285**, 88 (1999).
[4] S. H. Pan, J. P. O'Neal, R. L. Badzey, C. Chamon, H. Ding, J. R. Engelbrecht, Z. Wang, H. Eisaki, S. Uchida, A. K. Gupta, K.-W. Ng, E. W. Hudson, K. M. Lang, and J. C. Davis, Nature (London) **413**, 282 (2001).
[5] T. Cren, D. Roditchev, W. Sacks, and J. Klein, Europhys. Lett. **54**, 84 (2001).
[6] C. Howald, P. Fournier, and A. Kapitulnik, Phys. Rev. B **64**, 100504 (2001).
[7] K. M. Lang, V. Madhavan, J. E. Hoffman, E. W. Hudson, H. Eisaki, S. Uchida, and J. C. Davis, Nature (London) **415**, 412 (2002).
[8] J. E. Hoffman, K. McElroy, D.-H. Lee, K. M. Lang, H. Eisaki, S. Uchida, and J. C. Davis, Science **297**, 1148 (2002).
[9] O. Fischer, M. Kugler, I. Maggio-Aprile, C. Berthod, and C. Renner, Rev. Mod. Phys. **79**, 353 (2007).
[10] P. T. Sprunger, L. Petersen, E. W. Plummer, E. Lægsgaard, and F. Besenbacher, Science **275**, 1764 (1997); L. Petersen, P. T. Sprunger, P. Hofmann, E. Laegsgaard, B. G. Briner, M. Doering, H. P. Rust, A. M. Bradshaw, F. Besenbacher, and E. W. Plummer, Phys. Rev. B **57**, R6858 (1998).
[11] A. Weismann, M. Wenderoth, S. Lounis, P. Zahn, N. Quaas, R. G. Ulbrich, P. H. Dederichs, and S. Blügel, Science **323**, 1190 (2009). These authors pinpoint scatterers but using spatial rather than energy oscillations.
[12] K. McElroy, R. W. Simmonds, J. E. Hoffman, D.-H. Lee, J. Orenstein, H. Eisaki, S. Uchida, and J. C. Davis, Nature (London) **422**, 592 (2003); T. Hanaguri, Y. Kohsaka, J. C. Davis, C. Lupien, I. Yamada, M. Azuma, M. Takano, K. Ohishi, M. Ono, and H. Takagi, Nat. Phys. **3**, 865 (2007).
[13] Q.-H. Wang and D.-H. Lee, Phys. Rev. B **67**, 020511 (2003)
[14] This is analogous to the oscillations in Gutzwiller's trace formula in terms of the (classical) return times of a wave packet. See M. C. Gutzwiller, *Chaos in Classical and Quantum Mechanics* (Springer, New York, 1990).
[15] V. Heine, in *Solid State Physics*, edited by H. Ehrenreich, F. Seitz, and D. Turnbull (Academic Press, New York, 1980), Vol. 35; R. Haydock, *Solid State Physics* (Academic Press, New York, 1980).
[16] K. McElroy, J. Lee, J. A. Slezak, D.-H. Lee, H. Eisaki, S. Uchida, and J. C. Davis, Science **309**, 1048 (2005).
[17] D. R. Griffin, Science **100**, 589 (1944).
[18] A. V. Balatsky, I. Vekhter, and J.-X. Zhu, Rev. Mod. Phys. **78**, 373 (2006).
[19] If the contour included a point with $v_g[\vec{k}_\epsilon(s)]=0$, that point might also make a singular contribution.
[20] N. Bleistein and R. Handelsman, *Asymptotic Expansions of Integrals* (Dover, New York, 1975).
[21] G. Litak, P. Miller, and B. L. Gyorffy, Physica C **251**, 263 (1995).

[22] The (1,1) direction was chosen to bring out the difference in the two quasiparticle velocities most clearly. Along other directions, there are two velocities but they are very similar in magnitude and, hence, it is difficult to distinguish the two different wiggles. For this reason, possibly in a real experiment, one might have to look for echoes in certain directions.

[23] T. S. Nunner, W. Chen, B. M. Andersen, A. Melikyan, and P. J. Hirschfeld, Phys. Rev. B **73**, 104511 (2006).

[24] We used *s*-wave anomalous point impurity since it is quite straightforward to evaluate the T matrix for a local point impurity and we can compare it reliably to a local ordinary impurity. The argument should carry over for longer range ordinary and s/d-wave anomalous impurities because it rests on the comparison of the identity term and the GU term in the denominator of the T matrix irrespective of the structure of GU. The GU term will become nonlocal for nonlocal impurities but in the unitary limit, we will still have $T(\text{nonlocal};\omega)=G_0(\text{nonlocal};\omega)^{-1}$ where by nonlocal in the arguments, we mean the nonlocality of the impurity, be it ordinary or anomalous.

[25] G. Li, A. Luican, and E. Y. Andrei, Phys. Rev. Lett. **102**, 176804 (2009).

[26] Y. Kohsaka, C. Taylor, P. Wahl, A. Schmidt, J. Lee, K. Fujita, J. W. Alldredge, K. McElroy, J. Lee, H. Eisaki, S. Uchida, D.-H. Lee, and J. C. Davis, Nature (London) **454**, 1072 (2008).

[27] In this paper, we illustrated echolocation only for the case of *isolated* pointlike impurities. Real STM data will typically contain a superposition of LDOS wiggles from several nearby impurities; it is necessary (and not too difficult) for the analysis method to separate these contributions.